Science of the Total Environment 637–638 (2018) 1480–1491

Contents lists available at ScienceDirect

Science of the Total Environment

journal homepage: www.elsevier.com/locate/scitotenv

# The surprising recovery of red spruce growth shows links to decreased acid deposition and elevated temperature

Alexandra M. Kosiba [a,*], Paul G. Schaberg [b], Shelly A. Rayback [c], Gary J. Hawley [a]

[a] The University of Vermont, Rubenstein School of Environment and Natural Resources, Burlington, VT 05405, USA
[b] Forest Service, U.S. Department of Agriculture, Northern Research Station, Burlington, VT 05405, USA
[c] The University of Vermont, Department of Geography, Burlington, VT 05405, USA

## HIGHLIGHTS

- Following decline, this work suggests a recovery for red spruce trees.
- Higher temperatures outside the growing season were related to increased growth.
- N-deposition was associated with lower growth, but this has lessened over time.
- Growth relationships with predictor variable were inconstant through time.

## GRAPHICAL ABSTRACT

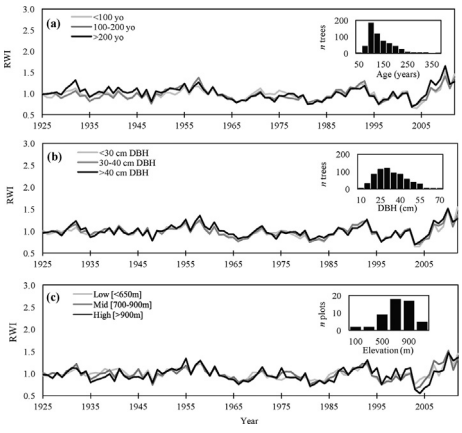


## ARTICLE INFO

*Article history:*
Received 7 January 2018
Received in revised form 26 April 2018
Accepted 1 May 2018
Available online 22 May 2018

Editor: Elena PAOLETTI

*Keywords:*
*Picea rubens*
Acid deposition
Nitrate
Dendrochronology
Woody growth
Climate change
Winter temperature

## ABSTRACT

Following growth declines and increased mortality linked to acid deposition-induced calcium depletion, red spruce (*Picea rubens* Sarg.) in the northeastern United States are experiencing a recovery. We found that more than 75% of red spruce trees and 90% of the plots examined in this study exhibited increasing growth since 2001. To understand this change, we assessed the relationship between red spruce radial growth and factors that may influence growth: tree age and diameter, stand dynamics, plot characteristics (elevation, slope, aspect, geographical position), and a suite of environmental variables (temperature, precipitation, climate and precipitation indices (degree days, SPEI [standardized precipitation evapotranspiration index], and acid deposition [$SO_4^{2-}$, $NO_3^-$, pH of rainfall, cation:anion ratio of rainfall]) for 52 plots (658 trees) from five states (spanning 2.5°N × 5°W). Examining the growth relationships from 1925 to 2012, we found that while there was variability in response to climate and acid deposition (limited to 1980–2012) by elevation and location, plot and tree factors did not adequately explain growth. Higher temperatures outside the traditional growing season (e.g., fall, winter, and spring) were related to increased growth. Nitrogen deposition (1980–2012) was associated with lower growth, but the strength of this relationship has lessened over time. Overall, we predict sustained favorable conditions for red spruce in the near term as acid deposition continues to decline and non-traditional growing season (fall through spring) temperatures moderate, provided that overall temperatures and precipitation remain adequate for growth.
© 2018 Elsevier B.V. All rights reserved.

* Corresponding author.
*E-mail addresses:* akosiba@uvm.edu, (A.M. Kosiba), pschaberg@fs.fed.us, (P.G. Schaberg), srayback@uvm.edu, (S.A. Rayback), gary.hawley@uvm.edu (G.J. Hawley).

https://doi.org/10.1016/j.scitotenv.2018.05.010
0048-9697/© 2018 Elsevier B.V. All rights reserved.

## 1. Introduction

Beginning in the mid-1960s, red spruce (*Picea rubens* Sarg.) in the northeastern United States (US) began to suffer from needle damage, crown deterioration, reductions in growth, and increased mortality (Johnson et al., 1988; McLaughlin et al., 1987; Scott et al., 1984). In the following decades, red spruce decline became one of the most intensively studied examples of forest degeneration in the US (Eagar and Adams, 1992). Through these studies, red spruce decline was attributed to winter injury, provoked by acid deposition-induced calcium (Ca) depletion (DeHayes et al., 1999; Schaberg et al., 2000). A number of factors contribute to a severe winter injury event, including both predisposing stresses (e.g., weather events that reduced carbon [C] capture in the prior growing season, like drought or extreme temperature [T] stress) and inciting stresses (e.g., extreme minimum temperature [$T_{min}$] and/or winter freeze-thaw cycles) (Schaberg et al., 2011). Pollution controls were enacted through the Clean Air Act and subsequent amendments, resulting in declines in acidic deposition (Driscoll et al., 2001) (Fig. 1). However, red spruce winter injury persisted and a severe region-wide event occurred as recently as 2003 (Lazarus et al., 2004) (Fig. S1).

Therefore, it was unexpected to discover that red spruce in the northeastern US recently exhibited a prominent increase in radial growth (Kosiba et al., 2013). Although Kosiba et al. (2013) were the first to report this growth upturn, other studies have noted the phenomenon in red spruce stands from New England and northern New York (Engel et al., 2016; Kosiba et al., 2017; Wason and Dovciak, 2017). There is additional evidence that red spruce regeneration has increased since earlier inventories as well (Foster and D'amato, 2015; Van Doorn et al., 2011). However, to date, no investigations have examined the possible factors involved in the observed change in red spruce radial growth.

Red spruce has been likened to the proverbial "canary in a coal mine" for its high sensitivity to acid deposition relative to co-occurring tree species. This sensitivity has been ascribed to the species' marginal cold tolerance (DeHayes et al., 2001), comparably low genetic diversity (Hawley and DeHayes, 1994), and unique capacity to deharden and photosynthesize during the traditional dormant season when the air T is favorable (e.g., during January thaws) (Schaberg et al., 1998; Schaberg et al., 1995; Schwarz et al., 1997). However, dehardening can increase the susceptibility of foliage to injury when freezing T returns (DeHayes et al., 2001; Schaberg and DeHayes, 2000). While these adaptions have made red spruce particularly vulnerable to acid deposition, they may now afford the species a competitive advantage with climate change. The ability of red spruce to photosynthesize when air T is favorable could result in additional opportunities for photosynthesis as global T rises, particularly if those increases occur outside the traditional growing season (e.g., fall, winter, and early spring) when co-occurring species remain leafless or dormant.

In the northeastern US, climatic trends over the past decade have included anomalously higher fall, winter, and spring T (Kunkel et al., 2013; NOAA National Climatic Data Center, 2010), which would reduce the chance of foliar freezing injury for red spruce (C loss) and increase opportunities for photosynthesis (C gain). Concurrent with increasing T, atmospheric carbon dioxide ($CO_2$) concentrations have risen steadily. While some studies have reported a fertilization effect of elevated $CO_2$ on aboveground C sequestration (Ainsworth and Long, 2005; Salzer et al., 2009; Soule and Knapp, 2006), others have detected no change under experimentally elevated $CO_2$ concentrations (Liu et al., 2010), or noted only a short-term (e.g., 1 year) increase in radial growth (Norby et al., 2010). However, there has been limited research of such relationships under ambient forest conditions. If combined with reductions in acidic pollutant inputs, these factors could allow for an overall increase in C sequestration for red spruce trees. Further, considering the relatively uniform genetics of the species (DeHayes, 1992), red spruce may exhibit a more cohesive response to environmental change compared to other tree species.

Although the drivers of xylem growth are varied and complex, we examined three hypotheses to disentangle the possible factors affecting red spruce growth across five states where it is an important component of forested ecosystems. ($H_1$) Changes in climate, particularly expansions to the length of the growing season and higher T outside the traditional growing season (i.e., fall, winter, and spring), have simultaneously reduced the likelihood of foliar winter injury (C loss) and increased photosynthesis (C capture). ($H_2$) Reductions in pollution deposition have alleviated a predisposing stress that contributed to past declines and resulted in C losses. ($H_3$) Increases in $CO_2$ have allowed for higher C capture and growth. We also include data on stand dynamics and mortality rates as a context for observed growth changes.

It is likely, however, that recent growth increases of red spruce are the result of a complex interplay between multiple factors. Indeed, prior studies of the climatic drivers of red spruce growth showed a strong de-coupling of growth and climate relationships around the start of red spruce decline (Johnson et al., 1988; McLaughlin et al., 1987), suggesting that the trees were no longer responding to the same environmental cues as they had prior to increased acid loading.

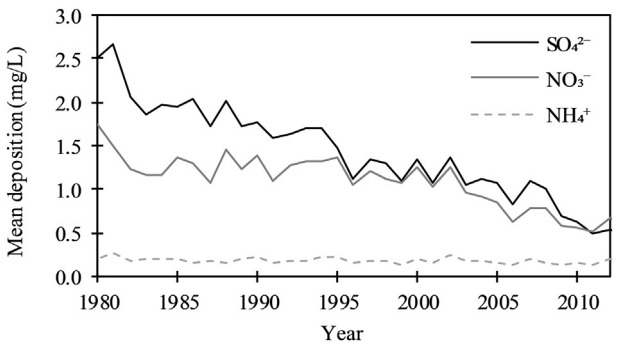


**Fig. 1.** Water year (previous Oct-current Sep) mean deposition (mg/L) of sulfate ($SO_4^{2-}$), nitrate ($NO_3^-$), and ammonium ($NH_4^+$) from seven air quality stations in the study region (see Table S2) (National Atmospheric Deposition Program, 2016).

## 2. Materials and methods

### 2.1. Study location

Red spruce tree cores were collected from five northeastern US states (NY, VT, NH, MA, and ME; study region extent: 42.67–45.04°N, 73.79–68.63°W) by the authors or affiliates (Engel et al., 2016; Kenefic, 2015; Kosiba et al., 2013; Kosiba et al., 2014; Pontius and Halman, 2012; Rayback, 2012; Wason et al., 2012; Weverka, 2012) (Fig. 2). Red spruce plots ($n = 52$) were included based on the strength of the common growth signal (i.e., r-bar; expressed population signal [EPS] > 0.80, see details below) (Table S1).

Plots were categorized by elevation (Low < 650 m [$n = 213$ trees], Mid 700–900 m [$n = 265$], and High > 950 m [$n = 180$]) to examine how landscape position that strongly affects weather and pollution deposition patterns in the region may also alter radial growth. Elevational groupings were separated by 50 m bands to assure that groupings were distinct. Plots encompassed a broad range in elevation, aspect, slope, mean tree age, and mean diameter at breast height (DBH, 1.37 m above ground level) (Table S1). While the region has experienced historic, widespread land-clearing and subsequent reforestation (Foster, 1992), we did not select plots based on stand age or DBH; rather, we attempted to obtain a range of tree ages and plot characteristics in

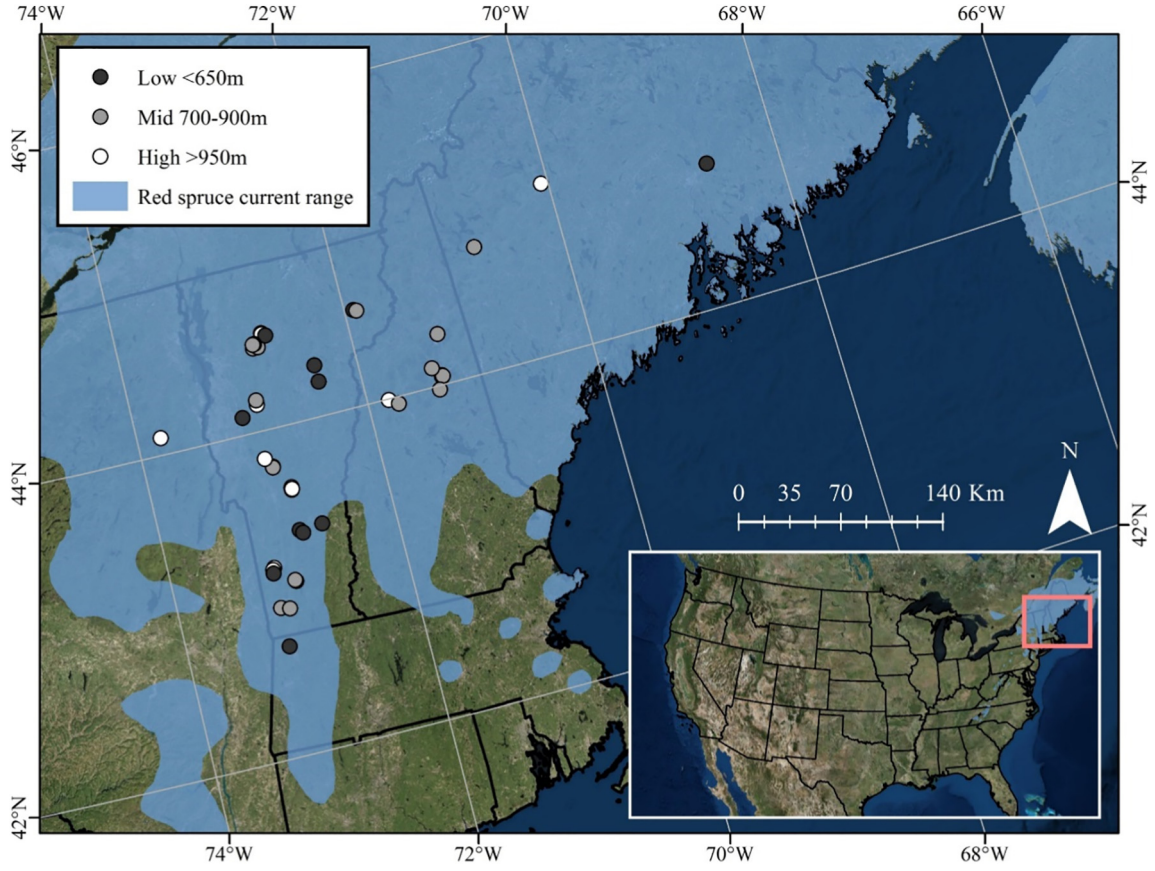


**Fig. 2.** Locations of red spruce (*Picea rubens* Sarg.) tree ring plots in NY, VT, NH, ME, and MA. Plots are designated by elevation (Low, Mid, and High) and overlaid on the current range of red spruce (blue shading) (U.S. Geological Survey, 1999). A total of 52 plots were sampled; adjacent plots appear overlapping and/or obscured in this representation.

order to characterize red spruce growth dynamics region-wide. Selected plots were not actively managed.

For the study area, the annual mean temperature ($T_{mean}$) is 6.3 °C. January is the coldest month (−7.5 °C average, 1925–2012) and July the warmest (19.4 °C) (Fig. S2) (NOAA National Centers for Environmental Information, 2016). An average of 106 cm of precipitation (P) is deposited uniformly throughout the year. In general, precipitation increases with elevation (NOAA National Centers for Environmental Information, 2016).

### 2.2. Dendrochronology

Dominant and codominant red spruce trees at the selected plots ($n = 661$ trees) were increment cored following standard dendrochronological techniques (Speer, 2010; Stokes and Smiley, 1996). We selected dominant and codominant red spruce for several reasons. First, these two crown classes are the most commonly selected for dendrochronological analyses and we were dependent on previously collected data for this study. Second, to test for the possible influence of declines in acid deposition, we selected those crown classes that were most affected by deposition inputs (Lazarus et al., 2004; Peart et al., 1991). Third, we were most interested in disentangling the climatic and environmental factors that affect red spruce across the region separate from the influences of light suppression. Due to the dominant influence of light suppression, intermediate and suppressed trees may exhibit less radial growth plasticity in response to climate compared to dominant and codominant trees (Martín-Benito et al., 2008). For most plots, at least nine trees closest to plot center were selected (see Table S1 for plot information), although some plots collected by our affiliates had fewer than nine trees. In this latter case, adjacent plots were combined to create a stronger common growth signal; this step was only necessary for four plots.

For all red spruce trees, two 5 mm increment cores were collected per tree at stem DBH, 180° to each other, and perpendicular to the dominant slope. Following collection, cores were air dried, mounted in grooved wooden blocks, and sanded with progressively finer grit sandpaper. Cores were visually crossdated using the list method (Yamaguchi, 1991) and microscopically measured to 0.001 mm resolution using a Velmex sliding stage unit (Velmex Inc., Bloomfield, NY) with MeasureJ2X software (VoorTech Consulting, Holderness, NH). We used COFECHA software (Holmes, 1983) to detect and correct for potential crossdating errors (Speer, 2010). To retain only accurately dated cores, individual cores were discarded if they were poorly correlated with the master chronology (i.e., below Pearson critical correlation level of 0.328 [99% confidence level]). This step was only used on a small number of cores (42 of 1320 cores) that we did not personally crossdate or were broken; in nearly all instances, the second core was retained for analysis. There were only three trees (of 661 original trees) where both cores were not useable, resulting in 658 trees for inclusion.

We calculated approximate tree age at breast height using the maximum number of rings per tree if pith was evident or estimated per core using a pith indicator (Speer, 2010) if pith had not been reached and pith location could be approximated based on the curvature of innermost rings. For incomplete cores where pith could not be estimated, or for those chronologies that were not in our possession, age was not assessed. Age was not assessable in 66 of the 658 trees. Trees were categorized into age and size (DBH) groups based on approximately equal sample sizes: <100 ($n = 240$ trees), 100–200 ($n = 193$), and >200 years ($n = 159$) old at breast height and <30 ($n = 232$), 30–40 ($n = 212$), and >40 cm DBH ($n = 214$).

We averaged raw ring width (RRW) by tree, then detrended, standardized, and prewhitened each series using the *dplR* package (Bunn et al., 2015) for R (Version 3.1.1) (R Development Core Team, 2016). We detrended with the Friedman Super Smoother (FSS) (tweeter = 5), a variable span smoother used to reduce the influence of disturbance on each series (Friedman, 1984; Pederson et al., 2013). We tested a variety of detrending methodologies, including using basal area increment, regional curve standardization, and cubic smoothing spines, among others (see Fig. S3). We found similar results regardless of methodology, and chose FSS based on the strength of the resulting statistics.

We developed chronologies at plot and regional scales, as well as aggregated by tree age-, tree size-, and plot elevation-class. Plot, and age- and size-class chronologies were calculated by aggregating individual tree chronologies with a Tukey's biweight robust mean. Regional and elevational chronologies were calculated as a mean of the plot chronologies. Detrended chronologies were standardized to a dimensionless index by dividing the observed by the expected value and stripped of temporal autocorrelation through autoregressive modeling to create prewhitened (residual) chronologies (RWI) (Cook, 1985). The residual chronologies are preferred for analysis because through the process of detrending, standardizing, and prewhitening, the remaining interannual variance can be attributed to exogenous factors (Cook and Peters, 1997).

Standard dendrochronological statistical parameters (Fritts, 1976; Wigley et al., 1984) were computed for each plot (Tables S1, S2). Specifically, from the RRW chronologies the parameters were series intercorrelation (SI), mean sensitivity (MS), mean value of tree-ring width (RW ± SD), first-order autocorrelation coefficient (AC), EPS, and signal to noise ratio (SNR). From the residual RWI chronologies, we computed the average correlation between individual series in a plot (r-bar), EPS, and SNR. All 52 resulting plot chronologies were truncated at the year when the EPS value fell below 0.80; for all plot-level chronologies this was 1925.

### 2.3. Growth trends

The slope of recent growth was computed using two start points (2001 and 2003) to the end of chronology or 2012, whichever came first (termed "recent growth trends") using RWI chronologies. The year 2001 was chosen as the start of the slope assessment because it captures recent growth increases while allowing for inclusion of the region-wide winter injury event (2003) with preceding years (2001, 2002), which is consistent with methods of Kosiba et al. (2013) and Engel et al. (2016). We also tested this relationship using 2003 as the start year for comparison. We tested the relationship between plot (e.g., slope, aspect, latitude, longitude, elevation, US State) and tree characteristics (approximate age, DBH) with recent growth trends for both time periods in a mixed effects model with "US state" as a random effect.

Potential disturbance events were detected two ways: (1) per tree using RRW following Fraver et al. (2009) using a 10-year running mean and an absolute threshold increase of 0.58 mm (a metric developed specifically for red spruce in the northeastern US); and (2) per plot using mean RRW following Lorimer and Frelich (1989) with a percent threshold of 60% and series threshold of 75%, over 10 years. In 2010, we also examined mortality in plots where we had quantified winter injury in 2004 (see Lazarus et al., 2004) (19 of the 52 plots in this study). The mortality rate was expressed as a per plot count of dead dominant or codominant red spruce that had been alive in 2003 to the total dominant and codominant red spruce in the plot. We examined if this 7-year mortality rate was positively correlated to the mean growth of surviving trees since 2003. We were not able to assess when the mortality occurred in this 7-year window, or the exact cause of the mortality; therefore, this analysis should be interpreted with these caveats in mind.

### 2.4. Climate, acid deposition, and atmospheric data

We averaged climate data (mean, maximum, and minimum monthly T [$T_{mean}$, $T_{max}$, $T_{min}$], and total monthly P; 1925–2012) from eight weather (meteorological) stations (NOAA Regional Climate Centers, 2016) (Table S2) in order to better characterize the regional climate over the spatial range of study plots and due to limitations in available data. From these, we computed seasonal (Winter: Dec-Feb, Spring: Mar-May, Summer: Jun-Aug, Fall: Sep-Nov) and water year (Wyr) (previous Oct- current Sep) values for the study region.

We included several climate indices in our analysis. We averaged the monthly indices of extreme T and P generated by NOAA for the same eight weather stations within the study region (NOAA National Centers for Environmental Information, 2016) (Table S2). These data included three measures of degree days: growing degree days (GDD, measured as cumulative degrees > 5 °C [41 °F]), cooling degree days (CDD, >18.3 °C [65 °F]) and heating degree days (HDD, <18.3 °C [65 °F]); indices of extreme heat (*n* days with $T_{max} \geq 32$ °C, extreme $T_{max}$) and cold (*n* days with $T_{min} \leq -18$ °C and ≤0 °C); and indices of extreme P (*n* days with ≥2.2 cm P, departure from normal P, total snowfall). From these, we computed seasonal and Wyr values. We also included the standardized precipitation-evapotranspiration index for the region (SPEI; a multi-scalar climatic drought index; version 3.23) at time scales of one, six (SPEI06 Apr-Sep), and nine (SPEI09 ending in Sep) months (National Drought Mitigation Center, 2012; Vicente-Serrano et al., 2010).

While CDD and HDD were derived for estimating building heating and cooling needs, respectively, prior research has shown that these metrics also relate to tree growth and physiology (Kosiba et al., 2017; Miller et al., 2014; Tyminski, 2011) and that they can be used as proxies for higher and lower T accumulation over time. While dendochronological assessments have traditionally utilized monthly T inputs, calendar distinctions are not based on tree physiology. In using an index that incorporates T accumulations over time, we hoped to detect stronger associations with tree growth.

To obtain an adequate temporal dataset of annual atmospheric $CO_2$ concentration for tree growth comparison (e.g., 1925–2012), we combined data from the Mauna Loa Observatory, HI, US (NOAA Earth System Research Laboratory Global Monitoring Division, 2016) and Law Dome, Antarctica ice core data (World Data Center for Paleoclimatology and NOAA Paleoclimatology Program, 2016). Lastly, we averaged pollutant deposition data ($SO_4^{2-}$, $NO_3^-$, $NH_4^+$, cation:anion ratio, and rainfall pH) from all National Atmospheric Deposition Program (NADP) stations within the study region (National Atmospheric Deposition Program, 2016) (Table S2). This dataset was limited to 1980–2012.

### 2.5. Comparisons of growth with climate and acid deposition data

To investigate the most influential factors that may explain red spruce growth trends from an initial list of dozens of variables, we used a three-step approach: (1) variable reduction using *treeclim*, (2) further variable reduction using stepwise linear regressions with AIC criteria, and (3) final model building and assessment. As we were interested in investigating if responses to environmental factors have changed over time, and some variables had a limited time span, we followed this three-step approach with four periods: the entire chronology 1925–2012; 1925–1960 (the period before acid deposition and red spruce decline (Driscoll et al., 2001); 1960–2012 (the period of peak acid deposition and red spruce decline (Driscoll et al., 2001) but lacking complete pollutant deposition data); and 1980–2012 (the period with pollutant deposition data). This method was first proposed to examine forest decline (Cook et al., 1987) rather than rebound, but is informative to identify changes in climate-growth relationships through time.

For variable reduction, we first used the package *treeclim* (Zang and Biondi, 2015) for R to assess the relationship between our suite of

selected climatic and environmental variables and standardized and detrended RWI over the current and previous year; this allowed us to examine the effect of the previous year's climate and pollution deposition on the following year's growth. *Treeclim* uses time-dependent bootstrapped resampling (1000 iterations) to test for linear correlations between the residual ring width data and each subvector of the climate matrix (Zang and Biondi 2015). Using *treeclim* as a first step allowed us to assess for any possible emergence of predictor variables that we would not have known *a priori* (Cook and Pederson, 2011) and to assist in variable selection for subsequent climate-growth models, which was important considering the large number of variables. To select the strongest relationships, variables were considered significant at the $\alpha = 0.01$ level.

Next, using the significant variables identified using *treeclim*, we calculated first differences of all input variables in order to remove trends and serial autocorrelation, as well as to enhance the magnitude of annual predictor variables. We limited inclusion to significant factors from the previous analysis and variables without significant multicollinearity. With this subset, we used stepwise linear regression, using AIC criteria, to further restrict linear model input variables.

Using this limited subset of possible predictor variables, we then created models of red spruce growth based on the four periods of interest. To assess change in model fit, we calculated the average reduction of error (RE) and coefficient of efficiency (CE). RE is a metric designed to assess the fit between the actual RWI data in the calibration and validation periods of the tree growth models and CE assess the fit between the actual and modeled data in the validation period. Both statistics range from $-\infty$ to $+1$ and a value $> 0$ validates the model fit (Cook et al., 1999). For both the 1925–2012 (entire time-period) and 1980–2012 (limited to pollution deposition record) models, we did not have a validation period to assess.

We first assessed the relationship between annual $CO_2$ concentrations and growth following the methods described above, but as $CO_2$ fertilization on tree growth may be masked by more variable environmental factors (e.g., T and P), we also assessed the relationship between $CO_2$ and the resultant residuals from each model (sensu Girardin et al., 2016). In doing so, we looked for trends not explained by the model parameters and regressed these values with $CO_2$. Lastly, we computed running correlations between the predicted and observed growth (methods follow Johnson et al., 1988), and between pollutant deposition and growth over time. To investigate possible spatial patterns between acid deposition and growth, we tested the fit of these models by elevational RWI chronologies.

## 3. Results

### 3.1. Growth trends and patterns

Red spruce trees in this study displayed a range of DBH (13–70.3 cm) and estimated age at breast height (41–373 years) (Fig. 3a, b). Most trees (78%) showed positive recent RWI growth (measured as slope of growth from 2001 to end of chronology), and it did not vary by DBH ($P = 0.55$, ANOVA) or age class ($P = 0.37$, Wilcoxon Rank Sum test due to unequal variances) (Fig. 3a, b). When aggregated, over 90% of the red spruce plots displayed positive, recent growth trends (Table S1). Plot locations encompassed an array of latitude/longitude, aspect, elevation (Figs. 2, 3), slope, and average tree age and DBH (Table S1). When we modeled RWI using fixed plot characteristics for the two time periods (2001–2012 and 2003–2012), no plot factors (e.g., mean DHB, mean age, elevation, aspect, slope) were significant in predicting recent growth.

Further, no major disturbance events were detected in individual trees or by plot since 1935 using either release detection method (Fig. 4). While Fig. 4 shows a peak in 2009 and 2010, this was only expressed in 18 out of 658 trees examined. Examining past data that we collected (see Kosiba et al., 2013), we found that 9.6% of trees that we evaluated for winter injury in 2003 and reassessed seven years later (2010) were dead; providing an overall mortality rate of 1.4% $yr^{-1}$. We looked at the relationship between recent RRW growth (assessed both as the slope of and as the mean growth from 2004 to 2010) and the mortality assessment per plot for a subset of plots for which we had prior data ($n = 19$), and found no relationship between the two factors ($R^2_{adj} = -0.04$, $P = 0.65$) (Fig. S5). By elevation group, the mean ± SE mortality was 9.9 ± 0.8% for high elevation plots, 9.1 ± 1.5% for mid elevation plots, and 9.5 ± 0.6% for low elevation plots. We did not detect significant differences in mortality among elevation groups (ANOVA, $P = 0.98$).

However, as these data were collected on a subset of 19 plots and we were not able to date the year of death, these results should be interpreted with caution. Nonetheless, these plots were disproportionately located at western and mid to high elevation locations that had higher winter injury in 2003 – so any release from injury-related mortality should have been greatest here, but it was not. Further, we did not find differences in growth based on tree DBH or estimated age at DBH, nor by elevation (Fig. 3).

### 3.2. Climate and acid deposition growth relationships

We found that various metrics of heat accumulation (e.g., degree days) were important for red spruce growth, particularly in the fall and spring seasons (Fig. 5). Both Wyr GDD (a measure of cumulative heat above 18.3 °C) and $T_{mean}$ were significantly related to growth ($r = 0.31$ and $r = 0.38$, $P \le 0.01$). Regionally, both of these metrics have remained statistically level ($P > 0.05$) since 1925 (NOAA National Weather Service, 2014) (Fig. S4). In the previous (p) November, measures of higher T ($T_{mean}$ and $T_{max}$) were associated with greater growth ($r = 0.38$ and 0.35, respectively; $P \le 0.01$), while lower T during this time (extreme $T_{min}$ e.g., <0 °C and <−18 °C) showed the opposite relationship ($r = -0.38$, $P \le 0.01$). Snow fall in pNov was also negatively correlated ($r = -0.23$, $P \le 0.01$), likely due to associated cloud cover. Similarly, reductions in heat accumulation in the spring were linked to reduced growth. April $T_{mean}$ and May cooling degree days (CDD) (a measure of heat accumulation > 18.3 °C) were positively associated with growth the following year ($r = 0.38$, $P \le 0.01$), while April HDD, a measure of cold, was negatively correlated to growth.

As expected, winter T was important for red spruce. Specifically, we found that higher winter and Jan $T_{mean}$ ($r = 0.33$ and 0.27, respectively; $P \le 0.01$), and higher Dec-Feb extreme $T_{min}$ ($r = 0.27$, 0.31, and 0.30, respectively; $P \le 0.01$), were positively associated with greater growth. Conversely, summer T demonstrated a complicated relationship between red spruce growth and T. While summer T was often positively associated with growth, pSummer T displayed the opposite relationship (Fig. 5). We found that high T in July (CDD, GDD, $T_{mean}$, and $T_{max}$) was negatively correlated with growth the subsequent year. However, during the summer of growth, red spruce shows a strong, positive association with Aug $T_{mean}$ ($r = 0.28$; $P \le 0.01$).

During summer, red spruce also displayed a greater sensitivity to pollution deposition than during the other seasons. Both $NH_4^+$ and $NO_3^-$ deposition in the summer were strongly, negatively correlated to growth the following year ($r = -0.60$ and $-0.53$, respectively; $P \le 0.01$) (Fig. 4). While we found that pH of rainwater and cation:anion ratio of deposition were both positively associated with red spruce growth ($P \le 0.05$) in our first step of our variable selection process, neither of these associations were strong enough to warrant inclusion in the final analysis.

Although not accounted for in our hypotheses, moisture availability was important for red spruce growth, particularly in antecedent years (Fig. 5). Both SPEI of pMay-Sept and pWyr P were associated with increases in growth ($r = 0.29$ and 0.34, respectively; $P \le 0.01$), but interestingly, we found that measures of extreme P, such as number of days with rainfall > 2.2 cm and overall departure from normal rainfall, had stronger correlations with growth ($r = 0.43$ and 0.44, respectively; $P \le$

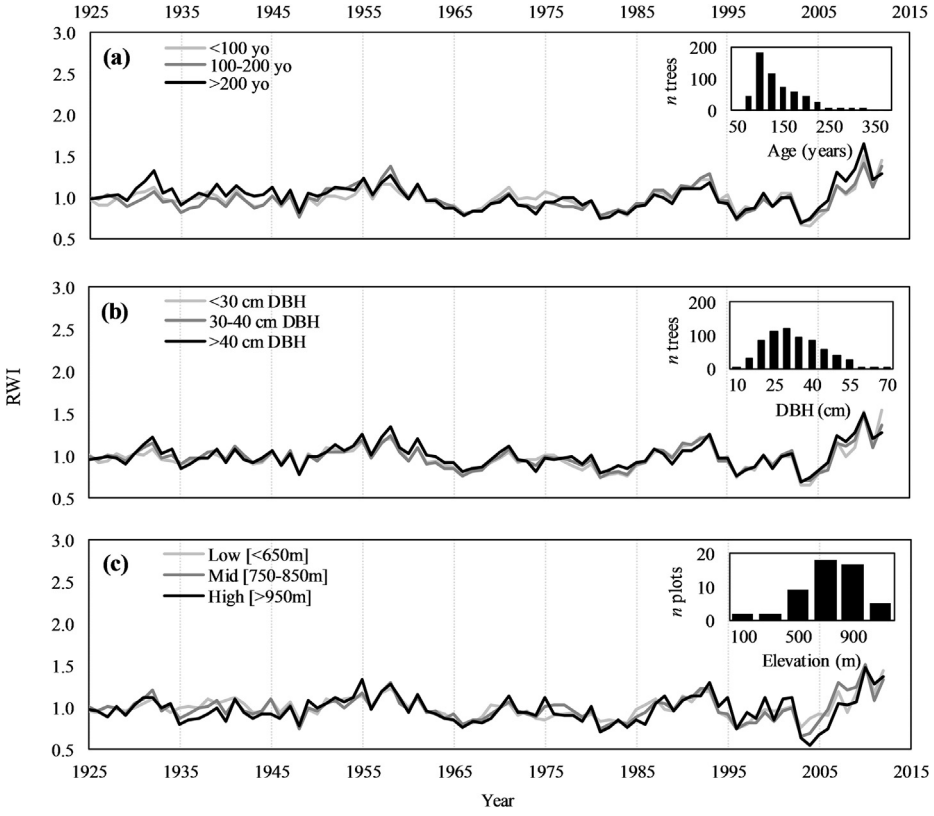


**Fig. 3.** Red spruce ring width index (RWI) chronologies classified by (a) estimated age (in years) at breast height (see Methods for details), (b) diameter at breast height (DBH; cm), and (c) plot elevation (Low < 650 m, Mid 700–900 m, High > 950 m). RWI chronologies for age and DBH class were created with a Tukey's biweight mean of individual tree series, while the elevation class chronology was created as a mean of plot chronologies. There were no significant differences between the chronologies based on age, DBH, or elevation class ($P = 0.37$, $P = 0.55$, and $P = 0.34$, respectively). Inset at upper right of chronologies displays the parameter distribution.

0.01). Examining these patterns over the seasons, we found strong, positive relationships between subsequent growth and spring and fall P (pMay and Nov extreme P, May P). If we couple these findings with the negative associations between growth and pSummer T, it indicates a drought response for the species. However, since extreme rainfall in the prior summer (e.g., pJuly) was associated with reduced growth, it may be that red spruce is more sensitive to low water availability during the spring and fall seasons, compared to summer. Lastly, we failed to find an association between $CO_2$ and red spruce growth using our variable selection process (both using *treeclim* or assessed on model residuals).

### 3.3. Growth models

Overall, the best model predictors for mean annual change in growth over the entire chronology ($RWI_{1925–2012}$, $R^2_{adj} = 0.60$, RMSE = 0.12, $P < 0.0001$) across the study area were Jan $T_{min}$ ($R^2_{adj} = 0.06$, $P = 0.0014$), pNov HDD ($R^2_{adj} = 0.14$, $P < 0.0001$), April GDD ($R^2_{adj} = 0.03$, $P < 0.0001$), pWyr P ($R^2_{adj} = 0.07$, $P = 0.0002$) and CDD ($R^2_{adj} = 0.31$, $P < 0.0001$) (Table 1, Fig. 6a). Of these predictors, pNov HDD and pWyr CDD had a negative association with growth, while the others were positively correlated with growth. Temperature preceding the growing season (e.g., pNov HDD, pWyr CDD, Jan $T_{min}$) explained 58% of the model variance, with pWyr P explaining 10%, and April GDD, 13%. The residuals of the climate models did not display a linear trend and further, did not have a significant correlation with $CO_2$ (Fig. S6).

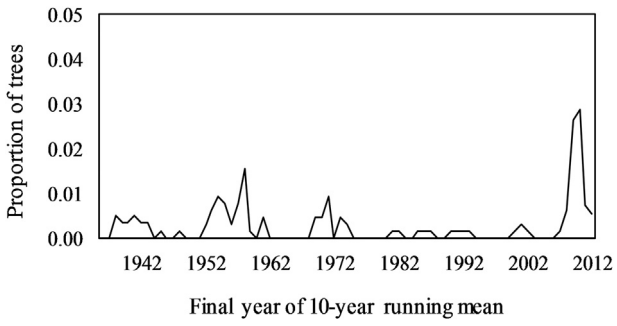


**Fig. 4.** Proportion of red spruce trees ($n = 658$) exhibiting a release event, assessed using a 10-year running mean following Fraver et al. (2009).

However, we found that predictor variables were not consistent through time or space (Table 1, Fig. 6). When we modeled growth using data before acid deposition-related decline ($RWI_{1925–1960}$), the model was not as strong at forecasting growth post-1960 (Adj. $R^2 = 0.58$, RMSE = 0.13, $P < 0.0001$; RE = 0.1, CE = 0.09) (Fig. 6b). Interestingly, this model only included T (i.e., April GDD, pWyr CDD, Jan $T_{min}$), while the three models using post-1960s data included pWyr P. A similar pattern emerged when we created a model of growth using only 1960 to 2012 data ($RWI_{1960–2012}$) and predicted pre-1960 growth (Fig. 6c; RE = 0.21, CE = 0.31). The $RWI_{1960–2012}$ model more accurately modeled recent growth trends (2001−2012) than the pre-1960 model. When we modeled growth to include pollutant deposition ($RWI_{1980–2012}$) (Fig. 6d), we found that a negative effect of pSummer $NO_3^-$ increased the model fit, particularly for recent growth ($r = 0.98$).

Running correlations between each model prediction and RWI show how these models failed to accurately predict growth through time (Fig. 7). For the three models that predicted growth from 1960 to 1980, there were sharp declines, and even reversals, in the correlation with RWI. The predicted $RWI_{1980–2012}$ model (that included $NO_3^-$ deposition) had a consistently strong fit, but due to the data limits of the acid deposition record, we could not assess the strength of this relationship pre-1980. Further, we found that the correlation between growth and $NO_3^-$ deposition was not consistent through time (1980–2012), even

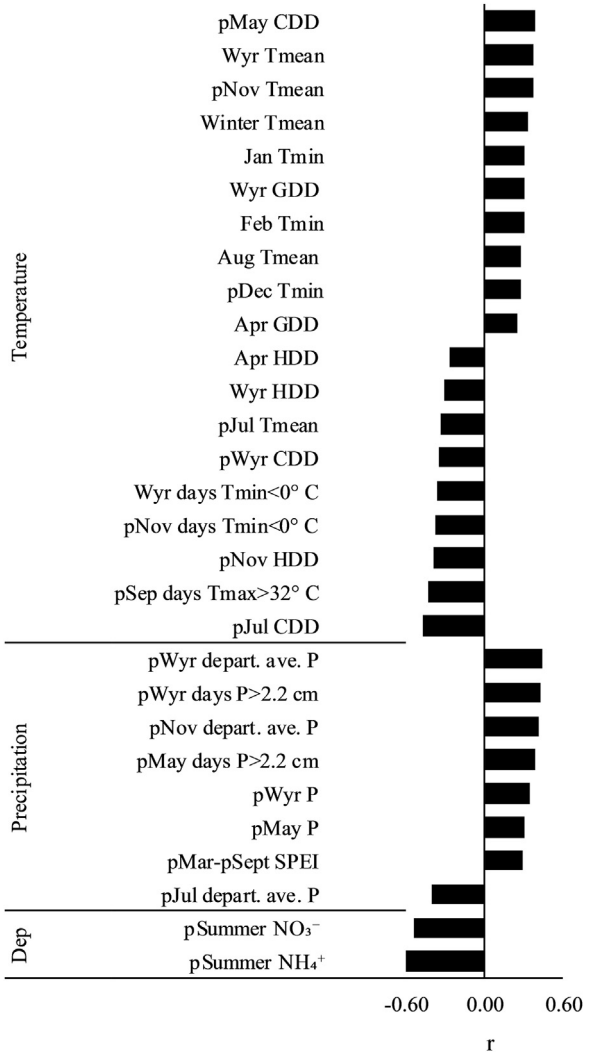


**Fig. 5.** Significant bootstrapped climate- and deposition-growth correlations (r) with mean RWI by variable type: temperature, precipitation, and atmospheric deposition (Dep). Coefficients were considered significant if $P \leq 0.01$. Abbreviations: p = previous year, N = number, Depart. = departure, T = temperature, P = precipitation, Min = minimum, GDD = growing degree days (cumulative degrees > 5 °C [41 °F]), HDD = heating degree days (cumulative days <18.3 °C [65 °F]), CDD = cooling degree days (cumulative degrees > 18.3 °C [65 °F]), Winter = previous December–February, SPEI = standardized precipitation evapotranspiration index, Wyr = water year (previous October to current September), $NO_3^-$ = nitrate deposition, $NH_4^+$ = ammonium deposition. For more information on variables see Methods.

for this limited dataset (Fig. 8). However, this analysis suggests that the strongly negative relationship between the two factors has decreased recently and may lead to more favorable conditions for the species.

As the $RWI_{1980–2012}$ model contained deposition data, which has been shown to increase with elevation (Mohnen, 1992), we tested this model with the three RWI elevation class chronologies. We saw differing response by elevation grouping (Table 2). All the model parameters imputed from the $RWI_{1980–2012}$ model were strong predictors of growth at Mid ($RWI_{Mid}$ $R^2_{adj} = 0.81$, RSME = 0.09, $P < 0.0001$) and High ($RWI_{High}$ $R^2_{adj} = 0.76$, RSME = 0.12, $P < 0.0001$) elevations, but not at Low elevation. Therefore, we used a reduced model for Low elevation. All elevation groups displayed a negative relationship with $NO_3^-$ deposition, but again, this relationship was stronger for Mid and High elevations ($RWI_{High}$ $R^2_{adj} = 0.47$, $P = 0.055$; $RWI_{Mid}$ $R^2_{adj} = 0.49$, $P = 0.015$, and $RWI_{Low}$ $R^2_{adj} = 0.36$, $P = 0.038$). For Low elevation, the other best predictor variables were the negative growth relationship with pNov HDD ($R^2_{adj} = 0.13$) and pJuly CDD ($R^2_{adj} = 0.11$).

## 4. Discussion

Here we presented the first comprehensive analysis of radial growth changes observed for red spruce trees in the northeastern US. While attributing cause and effect to *in situ* tree growth is challenging, we have identified significant correlations between growth and environmental variables, and have demonstrated that growth is synchronous across a wide spatial scale, suggesting that large-scale climate and pollutant deposition conditions have likely contributed to this growth surge.

### 4.1. Growth and temperature

Through this study, we demonstrated the complex relationship between tree growth and temperature (T). For example, higher summer T was negatively associated with subsequent growth, but positively associated with current growth (Fig. 5). There are a few possible reasons for this difference, which has also been reported for other conifer species (Girardin et al., 2016). Higher T could increase current-year growth if the tree favors consumption of C for short-term needs rather than for storage as non-structural carbohydrates to support growth the following year (Rennenberg et al., 2006). Further, T-induced increases in growth could result in the sequestration of other nutrients (e.g., N, Ca) that temporarily become limiting and indirectly suppress growth the following year (Rennenberg et al., 2006).

While negative relationships between high T and growth the following year suggest a legacy effect of higher T, conceivably through limitations of C or other compulsory elements, when combined with the strong positive relationship with P in the previous year, it could indicate that the species is sensitive to moisture availability. This was unexpected considering that the high moisture availability in the region (Pederson et al., 2013) that is projected to increase (Kunkel et al., 2013), but this time period does include a severe drought from 1962 to 1965 (Namias, 1966). Higher vapor pressure deficit has been shown to reduce both net photosynthesis and stomatal conductance in red spruce (Day, 2000).

Additionally, there is some evidence that acid deposition increases a tree's susceptibility to drought through a reduction in fine root biomass (Persson et al., 1995), which may partially explain the increase in strength of the relationship between growth and P after 1960 (Table 1). Moreover, for red spruce, it has been asserted that weather events in the preceding growing season that reduce C capture and nutrient uptake – for example drought – can predispose trees to winter injury (Schaberg et al., 2011), and thus cause reductions in growth due to C losses. However, for all analyses, we found that water availability (P, extreme P, SPEI) did not have as strong of an association or explain as much variance as T (Table 1), suggesting that T limits red spruce growth more than P for the period examined.

We also demonstrated the importance of favorable T outside the traditional growing season—fall, winter, and spring seasons (Fig. 5). Positive relationships between T during the spring and fall imply that low T restricted red spruce growth in these seasons. While extreme cold and heat in the fall can be detrimental to red spruce growth, favorable T could allow for an extended period for C capture. Further, a prolonged fall growing season could allow for more root elongation (Joslin and Wolfe, 1992), and increased water and nutrient uptake.

Similarly, we saw a positive relationship of growth with April GDD. At this time in the year, most deciduous hardwoods have not fully undergone leaf expansion; typically, that does not occur until May (Hufkens et al., 2012). Higher T in April that accumulate GDD (i.e., >5 °C), may confer a competitive advantage for red spruce trees, and perhaps other conifers (Girardin et al., 2016), that are able to rapidly increase photosynthetic activity compared to co-occurring species (DeHayes et al., 2001). Likewise, the physiological ability of red spruce to photosynthesize in the winter when T moderates (e.g., during winter thaws) could also confer a competitive advantage if winter T were favorable for photosynthesis. Aligning with previous findings (Johnson

**Table 1**
Model results (ANOVA, $P < 0.001$) predicting mean RWI for four time periods: predicted $RWI_{1925–2012}$ (Adj. $R^2 = 0.60$, RMSE = 0.12, $P < 0.0001$), the full chronology; predicted $RWI_{1925–1960}$, pre-acid deposition and red spruce decline (Adj. $R^2 = 0.58$, RMSE = 0.13, $P < 0.0001$); predicted $RWI_{1960–2012}$ (Adj. $R^2 = 0.78$, RMSE = 0.08, $P < 0.0001$); and predicted $RWI_{1980–2012}$, that included possible influences of pollutant deposition (pollution data limited to 1980–2012; Adj. $R^2 = 0.88$, RMSE = 0.07, $P < 0.0001$). Model terms, expressed as first differences, were first selected via bootstrapped correlation function analysis, stepwise linear regression, and assessment of collinearity. "Variance explained" is the partial proportion of variance explained by each factor. Note that pNov HDD has a negative relationship with RWI though the estimate was rounded to zero here.

| Time period for model construction | Term[a] | $R^2_{adj}$ | Estimate | SS | F Ratio | Prob > F | Variance explained |
|---|---|---|---|---|---|---|---|
| 1925–2012 | Jan $T_{min}$ | 0.06 | 0.005 ± 0.001 | 0.15 | 10.96 | 0.0014 | 8% |
| | pNov HDD | 0.14 | −0.000 ± 0.000 | 0.34 | 25.49 | <0.0001 | 18% |
| | April GDD | 0.03 | 0.002 ± 0.000 | 0.26 | 19.14 | <0.0001 | 13% |
| | pWyr P | 0.07 | 0.008 ± 0.002 | 0.20 | 14.71 | 0.0002 | 10% |
| | pWyr CDD | 0.31 | −0.001 ± 0.000 | 0.62 | 45.75 | <0.0001 | 32% |
| 1925–1960 | Jan $T_{min}$ | 0.002 | 0.006 ± 0.003 | 0.08 | 4.75 | 0.0372 | 10% |
| | April GDD | 0.33 | 0.003 ± 0.001 | 0.44 | 27.88 | <0.0001 | 58% |
| | pWyr CDD | 0.23 | −0.001 ± 0.000 | 0.20 | 12.46 | 0.0014 | 26% |
| 1960–2012 | Jan $T_{min}$ | 0.16 | 0.005 ± 0.001 | 0.08 | 12.83 | 0.0008 | 6% |
| | pNov $T_{mean}$ | 0.12 | 0.014 ± 0.003 | 0.17 | 27.23 | <0.0001 | 13% |
| | Aug $T_{max}$ | 0.32 | 0.010 ± 0.003 | 0.08 | 12.94 | 0.0008 | 6% |
| | April GDD | 0.004 | 0.001 ± 0.000 | 0.03 | 5.08 | 0.0291 | 2% |
| | pWyr P | 0.28 | 0.008 ± 0.002 | 0.13 | 20.06 | <0.0001 | 9% |
| | pWyr CDD | 0.36 | −0.001 ± 0.000 | 0.28 | 44.69 | <0.0001 | 21% |
| 1980–2012 | pNov HDD | 0.14 | −0.000 ± 0.000 | 0.06 | 14.13 | 0.0009 | 6% |
| | pJul CDD | 0.20 | −0.001 ± 0.000 | 0.12 | 27.20 | <0.0001 | 11% |
| | Jan $T_{min}$ | 0.06 | 0.010 ± 0.002 | 0.14 | 30.75 | <0.0001 | 13% |
| | pSummer $NO_3^-$ | 0.50 | −0.282 ± 0.072 | 0.07 | 15.46 | 0.0006 | 6% |
| | pWyr P | 0.07 | 0.007 ± 0.002 | 0.08 | 17.22 | 0.0003 | 7% |

[a] p = previous year, T = temperature, P = precipitation, Min = minimum, Max = maximum, GDD = growing degree days (cumulative degrees > 5 °C [41 °F]), HDD = heating degree days (cumulative days < 18.3 °C [65 °F]), CDD = cooling degree days (cumulative degrees > 18.3 °C [65 °F]), Summer: June–August, Wyr: water year, previous October to current September, $NO_3^-$: nitrate deposition. For more information on variables see Methods.

et al., 1988; McLaughlin et al., 1987), we saw that Jan $T_{min}$, the coldest month, was a strong predictor of growth, particularly for trees at both Mid and High elevations.

We established that both indices CDD (integrated heat exposure > 18.3 °C) and HDD (integrated cold exposure < 18.3 °C) were consistently associated with red spruce growth (Fig. 4). A strong relationship with CDD and radial growth has been found in other co-occurring tree species as well (Kosiba et al., 2017). While both CDD and HDD were established for building heating and cooling needs, because they are measures of T accumulation over a period, they may

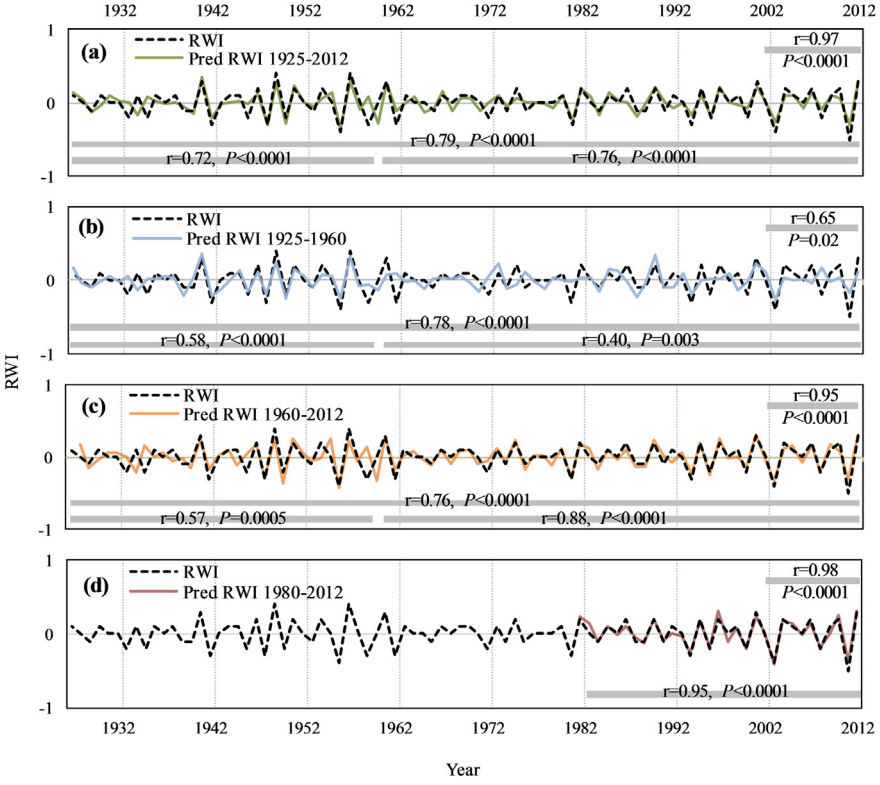


**Fig. 6.** First differences of observed mean red spruce tree ring chronologies (RWI, black dashed line) compared to predicted chronologies modeled using growth and climate data from four time periods: (a) predicted $RWI_{1925–2012}$ (Adj. $R^2 = 0.60$, RMSE = 0.12, $P < 0.0001$), the full chronology: (b) predicted $RWI_{1925–1960}$ (Adj. $R^2 = 0.58$, RMSE = 0.13, $P < 0.0001$), before acid deposition and red spruce decline; (c) predicted $RWI_{1960–2012}$ (Adj. $R^2 = 0.80$, RMSE = 0.08, $P < 0.0001$); and (d) predicted $RWI_{1980–2012}$ (Adj. $R^2 = 0.88$, RMSE = 0.07, $P < 0.0001$), the most recent growth and period of pollutant deposition data. Correlations (r) between the RWI chronologies and the predicted chronologies a–d and associated *P*-values are shown for different time periods (indicated with grey horizontal band).

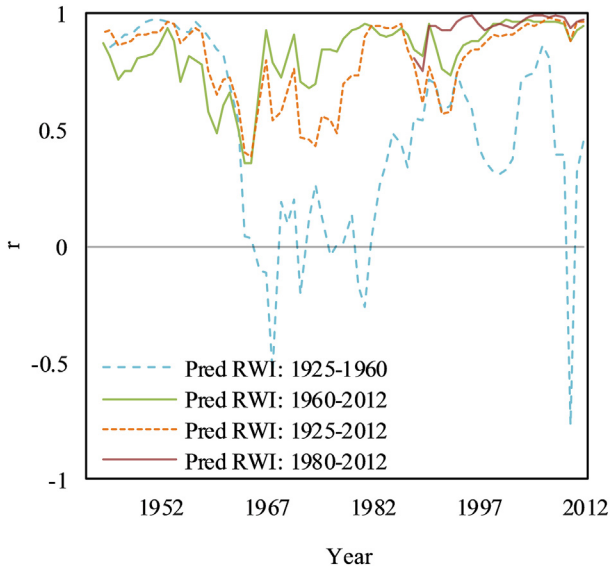


**Fig. 7.** Seven-year running Pearson's product moment correlations between mean RWI and predicted (pred) RWI based on four models. Dotted grey line demarks the threshold for significant positive correlations ($P < 0.05$). Methods follow Johnson et al., 1988.

have a stronger connection to tree physiology than traditional climate-growth metrics, like monthly $T_{mean}$. Previous investigations on the photosynthetic capacity of red spruce have established that rates peaked when air T was between 15 and 20 °C, and at higher air T respiration increased and water use efficiency decreased (Alexander et al., 1995); this may support the finding that greater CDD was negatively related to growth the following year.

These results support the hypothesis that heat accumulation outside the traditional growing season (e.g., fall, winter, early spring) positively relate to red spruce growth ($H_1$). If we continue to observe increasing T in these seasons, conditions may be favorable for the species. However, as the magnitude of the negative relationship between growth and pJuly T was larger than the positive relationship with Aug T (Fig. 5), the net effect could be an overall negative effect of higher summer T on growth. Therefore, rising T outside the summer may be beneficial, but increases during the summer months may be detrimental to growth.

### 4.2. Growth and acid deposition

Considering the plethora of research on the impact of acid deposition on red spruce growth and vigor (DeHayes et al., 1997; Engel et al., 2016; Schaberg et al., 2001), we were not surprised to find a strong, negative correlation between N-deposition and growth in the subsequent year. N-deposition in the summer likely created nutrient imbalances approaching winter when Ca, in particular, is needed for winter cold tolerance (Schaberg et al., 2001). However, the negative correlation between growth and $NO_3^-$ has lessened over time (Fig. 8), providing support for $H_2$. Unfortunately, the instrumental collection of acid deposition data began in the late 1970s, after acid deposition related decline in red spruce was already evident (Johnson et al., 1988). Thus, acid deposition cannot be included in our long-term growth models and we cannot assess how increases – as opposed to contemporary decreases – in acid deposition may have impacted red spruce growth.

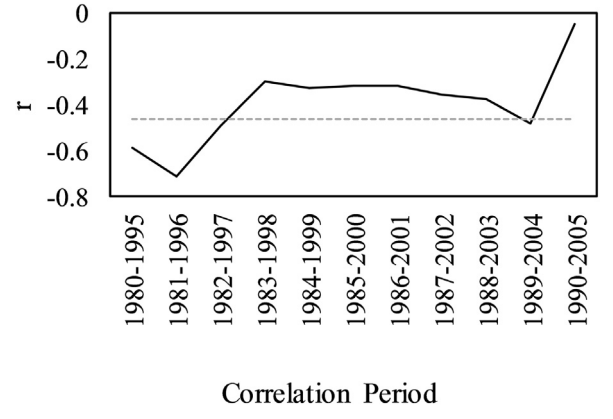


**Fig. 8.** Running 15-year bootstrapped correlations between RWI and previous year's $NO_3^-$ deposition from 1980 to 2012. Values below the grey, dotted line indicate a significant negative correlation ($P < 0.05$).

It has been shown that acid deposition within the range that has been encountered in the study region can increase the availability of soil-bound and toxic aluminum (Al), decrease accessibility of Ca (Joslin and Wolfe, 1992; Persson et al., 1995), and reduce mycorrhizal associations (Reich et al., 1986), which can alter biomass (Park et al., 2008) and nutrient uptake of fine roots (Persson et al., 1995). Taken together, these impacts could reduce C availability through reductions in water and nutrient uptake, and thus, retard C allocation to radial growth. Chronic N deposition has been identified as especially problematic to alterations in C allocation by reducing fine root biomass and critical nutrient uptake (Persson et al., 1995).

Interestingly, we found the strongest negative associations with $NO_3^-$ deposition at Mid elevation, followed by High elevation. Low elevation trees displayed a weaker relationship with $NO_3^-$, which aligns with research demonstrating increasing acid deposition (Cogbill and Likens, 1974) and red spruce winter injury severity (Lazarus et al., 2006) with elevation. However, why Mid elevation red spruce showed a stronger growth relationship with $NO_3^-$ is unclear, but this relationship was also identified in previous work using pollution critical load and exceedance models (Engel et al., 2016). Nevertheless, we predict that as acid deposition continues to decline we should see fewer winter injury events and more C capture, particularly for Mid and High elevation locations where winter injury had been most severe in the past (Lazarus et al., 2006).

We were surprised that not all measures of acid deposition, particularly $SO_4^{2-}$, were significantly related to growth, but this may have to do with spatial variability and the long-term, accumulated legacy effects of acid deposition on tree growth (e.g., Engel et al., 2016) as opposed to year-to-year relationships we focused on here. One additional reason for the lack of relationship with $SO_4^{2-}$ may be the robust interaction between $NO_3^-$, cation leaching, and water flux reported by Joslin and Wolfe (1992). They found that $NO_3^-$ was more strongly associated with cation leaching in both organic and mineral soil layers and had more temporal variability than $SO_4^{2-}$. Further, during periods of low water flux, soil $NO_3^-$ concentration increased considerably, and decreased during high water flux. This effect was so strong that during periods of drought, $NO_3^-$ was found to be much more important on a charge equivalent basis than $SO_4^{2-}$ (Joslin and Wolfe, 1992). The interaction between $NO_3^-$ and rainfall may partially explain the strengthening positive relationship after 1960 between Wyr P and subsequent growth, as well as the positive relationships with measures of extreme rainfall (i.e., departure from average P, N days $P > 2.2$ cm) (Fig. 5). However, others have reported greater detrimental effects to red spruce – including larger reductions in cold tolerance – with application of $SO_4^{2-}$ compared to $NO_3^-$ (Cape et al., 1991; Jacobson et al., 1990).

### 4.3. Growth and $CO_2$

We failed to find an association between $CO_2$ and red spruce growth through various methods (e.g., annual RWI growth or residuals of growth after accounting for the effects of climate and deposition [Fig. S6]) and thus, detected no support for $H_3$. This lack of association aligns with others who have shown no significant effect of $CO_2$ on radial growth (Bader et al., 2013; Girardin et al., 2016; Körner et al., 2005).

**Table 2**
Predicted $RWI_{1980–2012}$ models by plot elevation class: High ($R^2_{adj} = 0.76$, RSME = 0.12, $P < 0.0001$), Mid ($R^2_{adj} = 0.81$, RSME = 0.09, $P < 0.0001$), and Low ($R^2_{adj} = 0.50$, RSME = 0.12, $P < 0.0001$). All variables were converted into first differences prior to model building. "Variance explained" is the partial proportion of variance explained by each factor.

| Elevation class | Term[a] | Estimate ± SE | $R^2_{adj}$ | SS | F ratio | Prob > F | Variance explained |
|---|---|---|---|---|---|---|---|
| High (>950 m) | pSummer $NO_3^-$ | −0.256 ± 0.127 | 0.47 | 0.06 | 4.05 | 0.0551 | 4% |
| | pWyr P | 0.011 ± 0.003 | 0.13 | 0.16 | 11.42 | 0.0024 | 11% |
| | pJul CDD | −0.002 ± 0.000 | 0.11 | 0.22 | 15.70 | 0.0005 | 15% |
| | pNov HDD | −0.001 ± 0.000 | 0.11 | 0.09 | 6.34 | 0.0186 | 6% |
| | Jan $T_{min}$ | 0.006 ± 0.002 | 0.07 | 0.09 | 6.54 | 0.017 | 6% |
| Mid (700–900 m) | pSummer $NO_3^-$ | −0.266 ± 0.122 | 0.49 | 0.06 | 6.79 | 0.0152 | 5% |
| | pJul CDD | −0.001 ± 0.000 | 0.21 | 0.11 | 13.09 | 0.0013 | 10% |
| | pNov HDD | −0.001 ± 0.000 | 0.14 | 0.11 | 12.98 | 0.0014 | 10% |
| | pWyr P | 0.009 ± 0.002 | 0.06 | 0.12 | 14.01 | 0.001 | 10% |
| | Jan $T_{min}$ | 0.006 ± 0.002 | 0.05 | 0.09 | 11.10 | 0.0027 | 8% |
| Low (<650 m) | pSummer $NO_3^-$ | −0.266 ± 0.07 | 0.36 | 0.07 | 4.78 | 0.0377 | 14% |
| | pNov HDD | −0.001 ± 0.000 | 0.13 | 0.13 | 8.37 | 0.0075 | 25% |
| | pJul CDD | −0.001 ± 0.000 | 0.11 | 0.10 | 6.74 | 0.0151 | 20% |

[a] p = previous year, T = temperature, P = precipitation, Min = minimum, HDD = heating degree days (cumulative days < 18.3 °C [65 °F]), CDD = cooling degree days (cumulative degrees > 18.3 °C [65 °F]), Summer = Jun–Aug, Wyr: water year, previous October to current September, $NO_3^-$: nitrate deposition. For more information on variables see Methods.

There is considerable debate if elevated $CO_2$ will provoke physiological changes in trees (Silva and Horwath, 2013) and it is a difficult relationship to properly assess *in situ*. However, there may have been other physiological changes provoked by increasing atmospheric $CO_2$ that we did not assess, such as an alteration in abundance of stomata or increase in water use efficiency, which may not result in an increase in C gain. While some analyses of forest growth and instrumental $CO_2$ records have also attempted to find a relationship with radial growth (Girardin et al., 2016), there is evidence that $CO_2$ effects are muted or nonexistent on plots where other environmental factors (e.g., T, P, and nutrients) are more limiting to growth than C availability (Körner, 2003; Saurer et al., 2014). Based on the strong associations between red spruce growth and climate measures that we reported here, we hypothesize that other factors, namely T, water accessibility, and nutrient leaching via acidifying agents, have been more limiting to red spruce radial growth than $CO_2$ availability.

### 4.4. Regional trends

Based on the range of tree ages and DBH, variety of plot locations and characteristics (Fig. 3, Table S1) and failure to detect substantial stand disturbances (Fig. 4) (even following the recent [2003] winter injury event [Fig. S5]), we feel confident that the trends depicted here are representative of the regional red spruce population. The mortality rates we found in a subset of plots did not differ by elevation and averaged 1.4% $yr^{-1}$, which aligns with rates found in stands of other shade-tolerant, late successional tree species (Lorimer et al., 2001). In the 1970s, mortality rates were higher than what we reported here (3.7% $yr^{-1}$, Siccama et al., 1982), yet a growth increase with similar or greater magnitude to the one observed recently is not evident (Fig. 3). Further, as we included all red spruce plots in this analysis, not only those exhibiting recent increases in growth (10% plots did not show positive growth trends since 2002), we propose that these findings are representative of dominant and codominant red spruce in the broader region.

While we did not assess soil nutrition, an analysis indicated that recent growth increases occurred regardless of the combination of plot nutrition and pollution inputs (assessed via Critical Load Exceedance models) (Engel et al., 2016) and other work has shown that soils have only just begun to recover from decades of acidic inputs (Lawrence et al., 2015; Lawrence et al., 2012). While we did not study intermediate and suppressed red spruce trees, we postulate that similar growth trends and response to climate would be seen in these trees, although with a more muted response due to the effects of competition (Martín-Benito et al., 2008).

## 5. Conclusions

Following decades of declines, this work suggests a recovery for red spruce trees in the northeastern US. With decreases in acid deposition (Fig. 1) and increases in favorable climatic conditions, the species' current growth increase should persist, at least in the short term, and particularly for stands at elevations over 700 m. Considering these results, we predict that with continued increases in fall, winter, and spring T, coupled with reductions in pollutant loading, red spruce trees may even increase C capture further – if summer T does not exceed physiological thresholds and P is not limiting.

While the near-term predictions for red spruce may be favorable, the species could be vulnerable to change in the future, due to its low genetic diversity, past region-wide decline, and high spatial synchrony in growth patterns. The uncertainty lies in how P and T regimes will change in the future. If moisture availability (e.g., annual P, extreme P) continues to increase in the northeastern US (see Fig. S4), red spruce may have adequate water for increased C capture. However, if extreme weather events, such as prolonged drought or periods of extreme T become more frequent (especially in the summer), C capture could be limited. Indeed, the USDA Forest Service Climate Change Atlas projects that red spruce habitat suitability will decrease into the future primarily due to increases in July T (Prasad et al. 2007–ongoing). More broadly, this work demonstrates the importance of scientific inquiry to identify ecological problems (here acid deposition-induced decline), policy decisions to mitigate those issues (the Clean Air Act and subsequent amendments), and evidence of resultant biological recovery.

## Acknowledgements

We thank Drs. Martin Dovciak (SUNY-ESF), Jane Foster (University of Vermont [UVM]), Andrea Lini (UVM), Carol Adair (UVM), and two anonymous reviewers for their thoughtful suggestions. We greatly appreciate those who shared red spruce tree ring data or cores for use in this study: Ben Engel (UVM), Josh Halman (UVM), Laura Kenefic (USDA Forest Service), Jen Pontius (UVM and USDA Forest Service), Jay Wason (SUNY-ESF), and Aiko Weverka (UVM). This research was supported by the USDA Forest Service Northern Research Station (16-JV-11242316-089), and by grants from the Northeastern States Research Cooperative project 028698 – Reference Award Number: 13-DG-11242307-041, the Forest Ecosystem Monitoring Cooperative (formally the Vermont Monitoring Cooperative) project 027554 - Reference Award Number: 06130-VMC-UVM-12, and USDA McIntire-Stennis Forest Research Program (1002300). This manuscript is a contribution of the Hubbard Brook Ecosystem Study. Hubbard Brook is part of the Long-Term Ecological Research network, which is supported by the National Science

Foundation. The Hubbard Brook Experimental Forest is operated and maintained by the USDA Forest Service (Newtown Square, PA).

## Appendix A. Supplementary data

Supplementary data to this article can be found online at https://doi.org/10.1016/j.scitotenv.2018.05.010.

## References


Ainsworth, E.A., Long, S.P., 2005. What have we learned from 15 years of free-air CO2 enrichment (FACE)? A meta-analytic review of the responses of photosynthesis, canopy properties and plant production to rising CO2. New Phytol. 165, 351–372.

Alexander, J.D., Donnelly, J.R., Shane, J.B., 1995. Photosynthetic and transpirational responses of red spruce understory trees to light and temperature. Tree Physiol. 15, 393–398.

Bader, M.K.F., Leuzinger, S., Keel, S.G., Siegwolf, R.T.W., Hagedorn, F., Schleppi, P., Körner, C., 2013. Central European hardwood trees in a high-CO2 future: synthesis of an 8-year forest canopy CO2 enrichment project. J. Ecol. 101, 1509–1519.

Bunn, A., Korpela, M., Biondi, F., Campelo, F., Merian, P., Qeadan, F., Zang, C., 2015. dplR: Dendrochronology Program Library in R. R Package Version 1.6.3. http://r-forge.r-project.org/projects/dplr/.

Cape, J.N., Leith, I.D., Fowler, D., Murray, M.B., Sheppard, L.J., Eamus, D., Wilson, R.H.F., 1991. Sulphate and ammonium in mist impair the frost hardening of red spruce seedlings. New Phytol. 118, 119–126.

Cogbill, C.V., Likens, G.E., 1974. Acid precipitation in the northeastern United States. Water Resour. Res. 10, 1133–1137.

Cook, E.R., 1985. A Time Series Analysis Approach to Tree Ring Standardization (Dendrochronology, Forestry, Dendroclimatology, Autoregressive Process). (Unpublished Ph. D. Dissertation). University of Arizona, Tucson, AZ.

Cook, E.R., Pederson, N., 2011. Uncertainty, emergence, and statistics in dendrochronology. Dendroclimatology. Springer, pp. 77–112.

Cook, E.R., Peters, K., 1997. Calculating unbiased tree-ring indices for the study of climatic and environmental change. The Holocene 7, 361–370.

Cook, E.R., Johnson, A.H., Blasing, T.J., 1987. Forest decline: modeling the effect of climate in tree rings. Tree Physiol. 3, 27–40.

Cook, E.R., Meko, D.M., Stahle, D.W., Cleaveland, M.K., 1999. Drought reconstructions for the continental United States. J. Clim. 12, 1145–1162.

Day, M.E., 2000. Influence of temperature and leaf-to-air vapor pressure deficit on net photosynthesis and stomatal conductance in red spruce (Picea rubens). Tree Physiol. 20, 57–64.

Dehayes, D.H., 1992. Winter injury and developmental cold tolerance of red spruce. In: Eagar, C., Adams, M.B. (Eds.), The Ecology and Decline of Red Spruce in the Eastern United States. Springer-Verlag New York Inc, New York, NY, USA, pp. 295–337.

DeHayes, D.H., Schaberg, P.G., Hawley, G.J., Borer, C.H., Cumming, J.R., Strimbeck, G.R., 1997. Physiological implications of seasonal variation in membrane-associated calcium in red spruce mesophyll cells. Tree Physiol. 17, 687–695.

DeHayes, D.H., Schaberg, P.G., Hawley, G.J., Strimbeck, G.R., 1999. Acid rain impacts on calcium nutrition and forest health. Bioscience 49, 789–800.

DeHayes, D.H., Schaberg, P.G., Strimbeck, G.R., 2001. Red spruce cold hardiness and freezing injury susceptibility. In: Bigras, F. (Ed.), Conifer Cold Hardiness. Kluwer Academic Publishers, Dordrecht, the Netherlands.

Driscoll, C.T., Lawrence, G.B., Bulger, A.J., et al., 2001. Acidic deposition in the northeastern United States: sources and inputs, ecosystem effects, and management strategies. Bioscience 51, 180–198.

Eagar, C., Adams, M.B., 1992. Ecology and Decline of Red Spruce in the Eastern United States. Springer-Verlag, New York.

Engel, B.J., Schaberg, P.G., Hawley, G.J., Rayback, S.A., Pontius, J., Kosiba, A.M., Miller, E.K., 2016. Assessing relationships between red spruce radial growth and pollution critical load exceedance values. For. Ecol. Manag. 359, 83–91.

Foster, D.R., 1992. Land-use history (1730–1990) and vegetation dynamics in central New England, USA. J. Ecol. 80, 753–771.

Foster, J.R., D'amato, A.W., 2015. Montane forest ecotones moved downslope in northeastern US in spite of warming between 1984 and 2011. Glob. Chang. Biol. 4497–4507.

Fraver, S., White, A.S., Seymour, R.S., 2009. Natural disturbance in an old-growth landscape of northern Maine, USA. J. Ecol. 97, 289–298.

Friedman, J.H., 1984. A Variable Span Smoother. Standford University (DTIC Document).

Fritts, H.C., 1976. Tree Rings and Climate. Academic Press, New York.

U.S. Geological Survey (1999) Digital Representations of Tree Species Range Maps from "Atlas of United States Trees" by Elbert L. Little, Jr. (and Other Publications). U.S. Department of the Interior (accessed 10 October 2016).

Girardin, M.P., Bouriaud, O., Hogg, E.H., et al., 2016. No growth stimulation of Canada's boreal forest under half-century of combined warming and CO2 fertilization. Proc. Natl. Acad. Sci. 113.52, E8406–E8414.

Hawley, G.J., DeHayes, D.H., 1994. Genetic diversity and population structure of red spruce (Picea rubens). Can. J. Bot. 72, 1778–1786.

Holmes, R.L., 1983. Computer-assisted quality control in tree-ring dating and measurement. Tree-Ring Bull. 43, 69–78.

Hufkens, K., Friedl, M.A., Keenan, T.F., Sonnentag, O., Bailey, A., O'keefe, J., Richardson, A.D., 2012. Ecological impacts of a widespread frost event following early spring leaf-out. Glob. Chang. Biol. 18, 2365–2377.

Jacobson, J.S., Heller, L.I., Yamada, K.E., Osmeloski, J.F., Bethard, T., Lassoie, J.P., 1990. Foliar injury and growth response of red spruce to sulfate and nitrate acidic mist. Can. J. For. Res. 20, 58–65.

Johnson, A., Cook, E., Siccama, T., 1988. Climate and red spruce growth and decline in the northern Appalachians. Proc. Natl. Acad. Sci. 85, 5369–5373.

Joslin, J., Wolfe, M., 1992. Red spruce soil solution chemistry and root distribution across a cloud water deposition gradient. Can. J. For. Res. 22, 893–904.

Kenefic, L., 2015. Red Spruce Tree Cores from the Penobscott Experimental Forest, Maine. USDA Forest Service.

Körner, C., 2003. Carbon limitation in trees. J. Ecol. 91, 4–17.

Körner, C., Asshoff, R., Bignucolo, O., et al., 2005. Carbon flux and growth in mature deciduous forest trees exposed to elevated $CO_2$. Science 309, 1360–1362.

Kosiba, A.M., Schaberg, P.G., Hawley, G.J., Hansen, C.F., 2013. Quantifying the legacy of foliar winter injury on woody aboveground carbon sequestration of red spruce trees. For. Ecol. Manag. 302, 363–371.

Kosiba, A.M., Schaberg, P.G., Hawley, G.J., Rayback, S.A., 2014. Using Dendroecological Techniques to Interpret the Response of Trees to Environmental Change at Vermont Monitoring Cooperative's Mount Mansfield Study Site. Vermont Monitoring Cooperative.

Kosiba, A.M., Schaberg, P.G., Rayback, S.A., Hawley, G.J., 2017. Comparative growth trends of five northern hardwood and montane tree species reveal divergent trajectories and response to climate. Can. J. For. Res. 47, 743–754.

Kunkel, K.E., Stevens, L.E., Stevens, S.E., et al., 2013. Regional Climate Trends and Scenarios for the US National Climate Assessment. Part 1. Climate of the Northeast U.S. NOAA Technical Report NESDIS 142-1.

Lawrence, G.B., Shortle, W.C., David, M.B., Smith, K.T., Warby, RaF, Lapenis, A.G., 2012. Early indications of soil recovery from acidic deposition in U.S. red spruce forests. Soil Sci. Soc. Am. J. 76, 1407–1417.

Lawrence, G.B., Hazlett, P.W., Fernandez, I.J., et al., 2015. Declining acidic deposition begins reversal of forest-soil acidification in the northeastern U.S. and eastern Canada. Environ. Sci. Technol. 49 (22), 13103–13111.

Lazarus, B.E., Schaberg, P.G., DeHayes, D.H., Hawley, G.J., 2004. Severe red spruce winter injury in 2003 creates unusual ecological event in the northeastern United States. Can. J. For. Res. 34, 1784–1788.

Lazarus, B.E., Schaberg, P.G., Hawley, G.J., DeHayes, D.H., 2006. Landscape-scale spatial patterns of winter injury to red spruce foliage in a year of heavy region-wide injury. Can. J. For. Res. 36, 142–152.

Liu, J.X., Zhou, G.Y., Zhang, D.Q., Xu, Z.H., Duan, H.L., Deng, Q., Zhao, L., 2010. Carbon dynamics in subtropical forest soil: effects of atmospheric carbon dioxide enrichment and nitrogen addition. J. Soils Sediments 10, 730–738.

Lorimer, C.G., Frelich, L.E., 1989. A methodology for estimating canopy disturbance frequency and intensity in dense temperate forests. Can. J. For. Res. 19, 651–663.

Lorimer, C.G., Dahir, S.E., Nordheim, E.V., 2001. Tree mortality rates and longevity in mature and old-growth hemlock-hardwood forests. J. Ecol. 89, 960–971.

Martín-Benito, D., Cherubini, P., Del Río, M., Cañellas, I., 2008. Growth response to climate and drought in Pinus nigra Arn. trees of different crown classes. Trees 22, 363–373.

Mclaughlin, S.B., Downing, D.J., Blasing, T.J., Cook, E.R., Adams, H.S., 1987. An analysis of climate and competition as contributors to decline of red spruce in high elevation Appalachian forests of the eastern United States. Oecologia 72, 487–501.

Miller, A.C., Woeste, K.E., Anagnostakis, S.L., Jacobs, D.F., 2014. Exploration of a rare population of Chinese chestnut in North America: stand dynamics, health and genetic relationships. AoB Plants 6, plu065.

Mohnen, V.A., 1992. Atmospheric deposition and pollutant exposure of eastern US forests. Ecology and Decline of Red Spruce in the Eastern United States. Springer, pp. 64–124.

Namias, J., 1966. Nature and possible causes of the northeastern United States drought during 1962–65. Mon. Weather Rev. 94, 543–554.

National Atmospheric Deposition Program (2016) NADP/NTN Monitoring. US Geological Survey (accessed 4 May 2016).

National Drought Mitigation Center, 2012. SPEI. University of Nebraska, Lincoln http://droughtatlas.unl.edu/About.aspx, Accessed date: 15 March 2015.

Noaa Earth System Research Laboratory Global Monitoring Division, 2016. Monthly Average Mauna Loa $CO_2$. http://www.esrl.noaa.gov/gmd/ccgg/trends/, Accessed date: 6 October 2016.

Noaa National Centers for Environmental Information, 2016. Monthly Global Summaries by Station. http://www.ncdc.noaa.gov/cdo-web/search, Accessed date: 18 August 2016.

Noaa National Climatic Data Center, 2010. State of the Climate: National Overview.

Noaa National Weather Service, 2014. Monthly total Growing Degree Days for Burlington, VT. http://www.weather.gov/btv/climo_gdd, Accessed date: 23 April 2014.

Noaa Regional Climate Centers, 2016. DROUGHT-ACIS: Single Station Temperature and Precipitation Data. http://drought.rcc-acis.org, Accessed date: 14 August 2016.

Norby, R.J., Warren, J.M., Iversen, C.M., Medlyn, B.E., Mcmurtrie, R.E., 2010. CO2 enhancement of forest productivity constrained by limited nitrogen availability. Proc. Natl. Acad. Sci. 107, 19368–19373.

Park, B.B., Yanai, R.D., Fahey, T.J., Bailey, S.W., Siccama, T.G., Shanley, J.B., Cleavitt, N.L., 2008. Fine root dynamics and Forest production across a calcium gradient in northern hardwood and conifer ecosystems. Ecosystems 11, 325–341.

Peart, D.R., Jones, M.B., Palmiotto, P.A., 1991. Winter injury to red spruce at Mount Moosilauke, New Hampshire. Can. J. For. Res. 21, 1380–1389.

Pederson, N., Bell, A.R., Cook, E.R., et al., 2013. Is an epic pluvial masking the water insecurity of the greater New York city region? J. Clim. 26 (4), 1339–1354.

Persson, H., Majdi, H., Clemensson-Lindell, A., 1995. Effects of acid deposition on tree roots. Ecol. Bull. 158–167.

Pontius, J., Halman, J.M., 2012. Red Spruce Tree Cores from the Bartlett Experimental Forest, NH. University of Vermont.

Prasad, A.M., Iverson, L.R., Matthews, S., Peters, M., 2007. A climate change atlas for 134 forest tree species of the eastern United States [database]. Retrieved from US Department of Agriculture, Forest Service website: http://www.nrs.fs.fed.us/atlas/tree (ongoing).

R Development Core Team, 2016. R: A Language and Environment for Statistical Computing. R Foundation for Statistical Computing, Vienna, Austria.

Rayback, S.A., 2012. Red Spruce Tree Cores from Sites in Vermont, New Hampshire, and Maine. University of Vermont.

Reich, P.B., Stroo, H.F., Schoettle, A.W., Amundson, R.G., 1986. Acid rain and ozone influence mycorrhizal infection in tree seedlings. J. Air Pollut. Control Assoc. 36, 724–726.

Rennenberg, H., Loreto, F., Polle, A., Brilli, F., Fares, S., Beniwal, R., Gessler, A., 2006. Physiological responses of forest trees to heat and drought. Plant Biol. 8, 556–571.

Salzer, M.W., Hughes, M.K., Bunn, A.G., Kipfmueller, K.F., 2009. Recent unprecedented tree-ring growth in bristlecone pine at the highest elevations and possible causes. Proc. Natl. Acad. Sci. 106, 20348–20353.

Saurer, M., Spahni, R., Frank, D.C., et al., 2014. Spatial variability and temporal trends in water-use efficiency of European forests. Glob. Chang. Biol. 20, 3700–3712.

Schaberg, P.G., DeHayes, D.H., 2000. Physiological and environmental causes of freezing injury to red spruce. In: Mickler, R.A., Birdsey, R.A., Hom, J.L. (Eds.), Responses of Northern U.S. Forests to Environmental Change. Springer-Verlag, New York, pp. 181–227.

Schaberg, P.G., Wilkinson, R.C., Shane, J.B., Donnelly, J.R., Cali, P.F., 1995. Winter photosynthesis of red spruce from three Vermont seed sources. Tree Physiol. 15, 345–350.

Schaberg, P.G., Shane, J.B., Cali, P.F., Donnelly, J.R., Strimbeck, G.R., 1998. Photosynthetic capacity of red spruce during winter. Tree Physiol. 18, 271–276.

Schaberg, P.G., DeHayes, D.H., Hawley, G.J., Strimbeck, G.R., Cumming, J., Murakami, P.F., Borer, C.H., 2000. Acid mist, soil Ca and Al alter the mineral nutrition and physiology of red spruce. Tree Physiol. 20, 73–85.

Schaberg, P.G., DeHayes, D.H., Hawley, G.J., 2001. Anthropogenic calcium depletion: a unique threat to Forest ecosystem health? Ecosyst. Health 7, 214–228.

Schaberg, P.G., Lazarus, B.E., Hawley, G.J., Halman, J.M., Borer, C.H., Hansen, C.F., 2011. Assessment of weather-associated causes of red spruce winter injury and consequences to aboveground carbon sequestration. Can. J. For. Res. 41, 359–369.

Schwarz, P.A., Fahey, T.J., Dawson, T.E., 1997. Seasonal air and soil temperature effects on photosynthesis in red spruce (Picea rubens) saplings. Tree Physiol. 17, 187–194.

Scott, J.T., Siccama, T.G., Johnson, A.H., Breisch, A.R., 1984. Decline of red spruce in the Adirondacks, New York. Bull. Torrey. Bot. Club 111, 438–444.

Siccama, T.G., Bliss, M., Vogelmann, H.W., 1982. Decline of red spruce in the green mountains of Vermont. Bull. Torrey. Bot. Club 109, 162–168.

Silva, L.C., Horwath, W.R., 2013. Explaining global increases in water use efficiency: why have we overestimated responses to rising atmospheric $CO_2$ in natural forest ecosystems? PloS one 8 (1), e53089.

Soule, P.T., Knapp, P.A., 2006. Radial growth rate increases in naturally occurring ponderosa pine trees: a late-20th century CO2 fertilization effect? New Phytol. 171, 379–390.

Speer, J.H., 2010. Fundamentals of Tree-Ring Research. Press, University of Arizona.

Stokes, M., Smiley, T., 1996. An Introduction to Tree-ring Dating. University of Chicago Press.

Tyminski, W.P.J., 2011. The Utility of Using Sugar Maple Tree-ring Data to Reconstruct Maple Syrup Production in New York. (Unpublished Ph.D). The University of North Carolina at Greensboro (154 pp).

Van Doorn, N.S., Battles, J.J., Fahey, T.J., Siccama, T.G., Schwarz, P.A., 2011. Links between biomass and tree demography in a northern hardwood forest: a decade of stability and change in Hubbard Brook Valley, New Hampshire. Can. J. For. Res. 41, 1369–1379.

Vicente-Serrano, S.M., Beguería, S., López-Moreno, J.I., 2010. A multiscalar drought index sensitive to global warming: the standardized precipitation evapotranspiration index. J. Clim. 23, 1696–1718.

Wason, J.W., Dovciak, M., 2017. Tree demography suggests multiple directions and drivers for species range shifts in mountains of northeastern United States. Glob. Chang. Biol. 23, 3335–3347.

Wason, J.W., Dovciak, M., Bier, C.M., Battles, J., 2012. Red Spruce Tree Cores from Dial Mountain, NY. SUNY-EFS.

Weverka, A.S., 2012. Remote sensing of productivity in northeastern forests. (MS Thesis). Unpublished Master's of Science Rubenstein School of Environment and Natural Resources. University of Vermont.

Wigley, T.M., Briffa, K.R., Jones, P.D., 1984. On the average value of correlated time series, with applications in dendroclimatology and hydrometeorology. Bull. Am. Meteorol. Soc. 23, 201–213.

World Data Center for Paleoclimatology and NOAA Paleoclimatology Program, 2016. Law Dome Ice Core Data.

Yamaguchi, D.K., 1991. A simple method for cross-dating increment cores from living trees. Can. J. For. Res. 21, 414–416.

Zang, C., Biondi, F., 2015. Treeclim: an R package for the numerical calibration of proxy-climate relationships. Ecography 38 (4), 431–436.